Location-adaptive transmission for indoor visible light communication*

WANG Chun-yue (王春悦)**, **WANG Lang** (王浪), **and CHI Xue-fen** (迟学芬)
College of Communication Engineering, Jilin University, Changchun 130012, China

(Received 23 October 2013; Revised 11 November 2015)

A location-adaptive transmission scheme for indoor visible light communication (VLC) system is proposed in this paper. In this scheme, the symbol error rate (*SER*) of less than 10^{-3} should be guaranteed. And the scheme is realized by the variable multilevel pulse-position modulation (MPPM), where the transmitters adaptively adjust the number of time slots n in the MPPM symbol according to the position of the receiver. The purpose of our scheme is to achieve the best data rate in the indoor different locations. The results show that the location-adaptive transmission scheme based on the variable MPPM is superior in the indoor VLC system.
Document code: A **Article ID:** 1673-1905(2016)01-0069-5
DOI 10.1007/s11801-016-5212-5

As an innovative technology, indoor visible light communication (VLC) has been a research hotspot in recent years[1,2]. T. Komine et al[3] proposed an indoor VLC system and stated that the multipath interference and reflection can affect the signal to noise ratio (*SNR*). Jupeng Ding[4,5] proposed an evolutionary algorithm based on optimization scheme to realize uniform received power on different locations. A. Burton et al[6] focused on adjusting receiver with varying field of view (FOV). And C. W. Chow[7] proposed an adaptive control of the orthogonal frequency division multiplexing (OFDM) modulation to maintain the VLC transmission performance. But the OFDM has a disadvantage of high peak-to-average power ratio (PAPR)[8]. In order to achieve a high data rate, some papers paid attention to design receiver[9,10]. However, these methods have either high complexity or high cost.

Ref.[11] presented a novel rate-adaptive transmission scheme using block coding of variable Hamming weight based on multiple pulse position modulation (MPPM) technique. And Ref.[12] proposed an digital pulse interval modulation (DPIM) for VLC, but it could not be adaptive control to maintain the indoor VLC transmission performance. In this paper, a location-adaptive transmission scheme for indoor VLC based on MPPM technique is presented.

In MPPM, the duration of each symbol $T_{symb}=1/R_{symb}$ is divided into n slots, and each slot has a duration of $T_{slot}=T_{symb}/n$. Suppose that we put M bit information mapping on n slots with r pulses, which expresses as (n, r) MPPM. A symbol is transmitted in r slots, thereby giving C_n^r possible symbols. Hence, the potential of encoding is $\log_2 C_n^r$ bits, thus a higher bandwidth efficiency is offered compared with that of the standard PPM scheme[13].

We first introduce the multiple-source light channel model, and demonstrate that the distribution of the *SNR* is nonuniform. Then we propose a location-adaptive transmission scheme in which the data rate is differently dependent on the position of the receiver. Finally, we apply variable MPPM to location-adaptive transmission, and get the proper (n, r) MPPM for the indoor location.

Fig.1 is the propagation model of line of sight (LOS), where ϕ is the angle of irradiance, ψ is the angle of incidence, d is the distance between a light-emitting diode (LED) and a detector, and Ψ_c denotes the width of the FOV at a receiver. In typical VLC scenario, the weight of directed light component in the total received power exceeds 95%[3]. The rate of the reflected light is small enough compared with that of directed light. Here, the rate of directed light is 95.16%, those of the first and the second reflected lights are 3.57% and 1.27%, respectively. Accordingly, we only consider the directed light for convenience of compute and analysis in this paper.

A room with size of 5.0 m×5.0 m×3.0 m is assumed. LED lights are installed at a height of 2.5 m from the floor. Fixtures in the room are arranged as shown in Fig.2. Each LED chip is filled with 3 600 (60×60) LEDs. The space between LED chips is 1 cm. Other conditions are summarized in Tab.1.

* This work has been supported by the Jinlin Provincial Science & Tenchology Department of China (No.20130413052GH).
** E-mail: wangchunyue1971@163.com

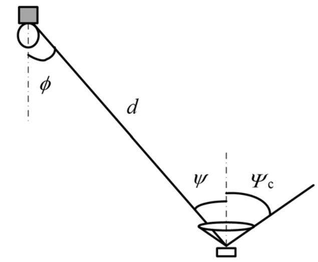

Fig.1 Propagation model of LOS

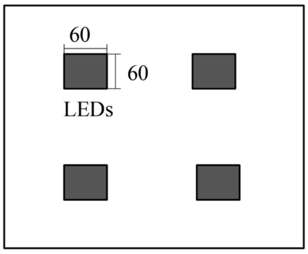

Fig.2 The position of LEDs on the ceiling

It is assumed that an LED chip has a Lambertian radiation pattern. Hence, the channel direct current (DC) gain is given as[14]

$$H(0)=\begin{cases}\frac{m+1}{2\pi d^2}A\cos^m(\phi)T_s(\psi)g(\psi)\cos(\psi), & 0\le\psi\le\Psi_c\\ 0, & \psi>\Psi_c\end{cases}, \quad (1)$$

where $T_s(\psi)$ is the gain of an optical filter, A is the physical area of the detector in a photodetector (PD), and m is the order of Lambertian emission which given by the semi-angle at half illumination of an LED $\Phi_{1/2}$ as

$$m=-\ln 2/\ln(\cos\Phi_{1/2}) . \quad (2)$$

The gain of an optical concentrator $g(\psi)$ can be given as

$$g(\psi)=\begin{cases}l^2/\sin^2\Psi_c, & 0\le\psi\le\Psi_c\\ 0, & \psi\ge\Psi_c\end{cases}, \quad (3)$$

where l is the refractive index.

In this paper, we assume that the noise is an additive white Gaussian noise (AWGN). The optical wireless channel model is expressed as[15]

$$y(t)=Rx(t)\otimes h(t)+n(t) , \quad (4)$$

where $y(t)$ represents the received signal current, $x(t)$ represents the transmitted optical pulse, $n(t)$ represents the AWGN noise, the symbol $\otimes$ denotes convolution, and R represents an optical/electrical (O/E) conversion efficiency at a user terminal's PD.

A non-directed LOS path is assumed in the paper. The channel is given as[3]

$$H(0)=\int_{-\infty}^{\infty}h(t)\mathrm{d}t . \quad (5)$$

Tab.1 The Parameters using in the simulation

Parameters	Values
Transmitted optical power (mW)	20
Semi-angle at half illumination $\Phi_{1/2}$ (°)	70
Size of LED light (m)	0.59×0.59
FOV at a receiver Ψ_c (°)	60
Physical area A of a PD (cm^2)	1.0
Refractive index of a lens at PD	1.5
Background current I_{bg} (μA)	5 100
Noise bandwidth factor I_2	0.526
Open-loop voltage gain G	10
Fixed capacitance η (pF/cm^2)	112
FET transconductance g_m (mS)	30
FET channel noise factor Γ	1.5
Symbol rate R_{symb} (MHz)	50
Absolute temperature T_k (K)	295
O/E conversion efficiency (A/W)	0.53

The received power is the sum of power from all the LEDs, which can be expressed as

$$P_r=\sum_{\text{LEDs}}H_i(0)P_t , \quad (6)$$

where the transmitted power P_t is

$$P_t=\lim_{T\to\infty}\frac{1}{2T}\int_{-T}^{T}X(t)\mathrm{d}t . \quad (7)$$

We consider the (2, 1) MPPM modulation scheme. And we compute the *SNR* at receiver with the slot rate of R_{slot} (R_{slot}=1/T_{slot}). The signal component S is

$$S=R^2P_{rsignal}^2 , \quad (8)$$

where $P_{rsignal}$ is the desired receive signal power :

$$P_{rsignal}=\int_0^{T_{slot}}\left(\sum_{i=1}^{\text{LEDs}}h_i(t)\otimes X(t)\right)\mathrm{d}t . \quad (9)$$

The Gaussian noise has a total variance N that is the sum of contributions from shot noise, thermal noise and inter-symbol interference (ISI) noise by an optical path difference[3]:

$$N=\sigma_{shot}^2+\sigma_{thermal}^2+R^2P_{risi}^2 , \quad (10)$$

where

$$P_{risi}=\int_{T_{slot}}^{\infty}\left(\sum_{i=1}^{\text{LEDs}}h_i(t)\otimes X(t)\right)\mathrm{d}t , \quad (11)$$

$$\sigma_{shot}^2=2qR(P_{rsignal}+P_{risi})B+2qI_{bg}I_2B , \quad (12)$$

$$\sigma^2_{\mathrm{thermal}} = \frac{8\pi k T_{\mathrm{k}}}{G}\eta A I_2 B^2 + \frac{16\pi^2 K T_{\mathrm{k}} \Gamma}{g_{\mathrm{m}}}\eta^2 A^2 I_3 B^3 , \quad (13)$$

where q is the electronic charge, B is equivalent noise bandwidth, and I_{bg} is background current which is assumed from direct sum light. The noise bandwidth factor is I_2=0.562, K is Boltzmann's constant, T_{k} is absolute temperature, G is the open-loop voltage gain, η is the fixed capacitance of PD per unit area, Γ is the field effect transistor (FET) channel noise factor, g_{m} is the FET transconductance, and I_3=0.086 8[16]. Fig.3 shows the influence of noise variance on slot rate in the position (2.5, 2.5, 0.85). We can see that the ISI noise is the main influence factor when the slot rate is less 10^{10} Hz. Besides, we can see from Fig.3 that the noise is increased with the increase of slot rate.

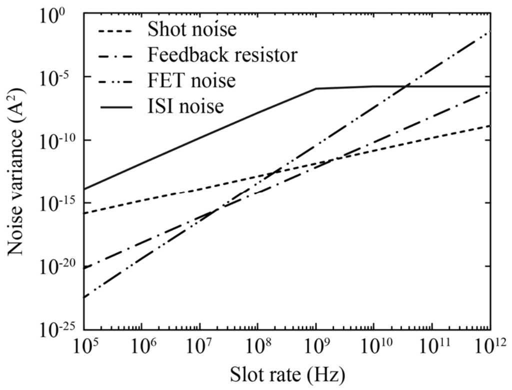

Fig.3 The influence of noise variance on slot rate

Fig.4 shows the distribution of the *SNR* by using (2, 1) MPPM. We can see that the distribution of *SNR* is non-uniform. There is about 10 dB difference between the maximum and the minimum. The maximum value of *SNR* is 23.855 4 dB, however the minimum is only 13.146 2 dB. Consequently, for achieving a data rate of every location communication as high as possible, we propose a location-adaptive transmission scheme in this paper.

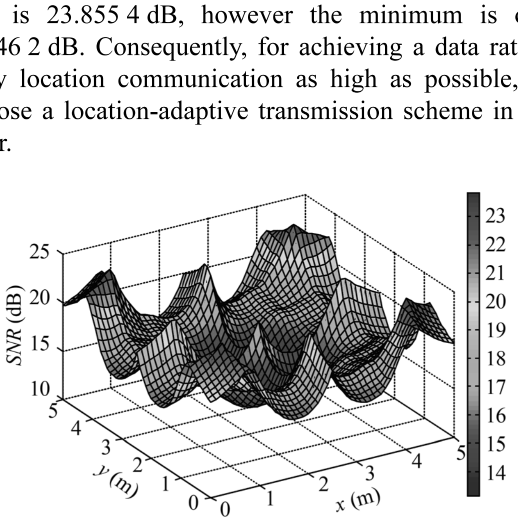

Fig.4 The distribution of *SNR* for (2, 1) MPPM

In the indoor office environment, with the purpose of avoiding flicker, the average transmitted power of a symbol should be constant. Thus, in a symbol duration T_{symb}, we assume r=n/2, which indicates that half of slots can have power pulse. In one symbol duration time T_{symb}, and (n, r) MPPM can transmit I bit of information as

$$I = \log_2 C_n^r . \quad (14)$$

We can see from Fig.5 that the information bits linearly increase as the increase of the number of slots. In addition, it shows that MPPM is a high efficiency modulation in indoor VLC system. In consequence, we apply the MPPM to the location-adaptive transmission scheme. We can transmit more information with higher (n, r) MPPM.

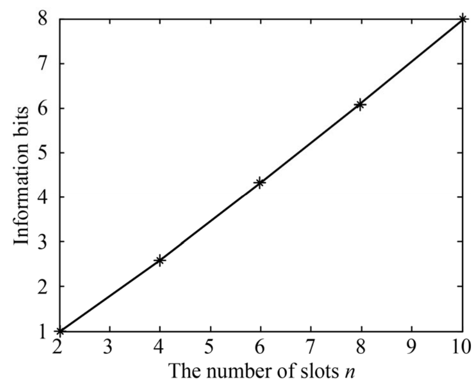

Fig.5 The information bits of (*n*, *r*) MPPM

Transmitters can transmit in a high speed by using a higher (n, r) MPPM in the location where the channel quality is superior. However, a higher (n, r) MPPM will result in a dreadful ISI noise which can be seen from Fig.3, and it will in turn decrease the *SNR*. As an example, Fig.6 shows the distribution of the *SNR* by using (4, 2) MPPM. Compare with the distribution of *SNR* by using (2, 1) MPPM as shown in Fig.4, we can know that the (4, 2) MPPM has a lower *SNR* under the same transmitted optical power. Because the (4, 2) MPPM has a higher slot rate which will trigger ISI more seriously. Hence, it is difficult to choose a proper (n, r) MPPM in a location.

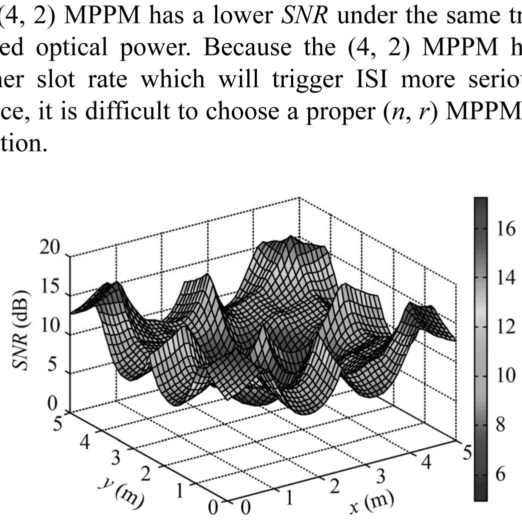

Fig.6 The distribution of *SNR* for (4, 2) MPPM

To get a proper (n, r) MPPM, we first analyze the symbol error rate (*SER*) of (n, r) MPPM. An MPPM symbol has n slots, and there will be some error if any slot of the symbol has error. Thus, the *SER* of the (n, r) MPPM can be express as

$$P_s = 1-(1-P_e)^n \,, \tag{15}$$

where P_e is the error rate of a slot. "1" represents that there is pulse, on the other hand, "0" represents that there is no pulse. The number of "1" equal to that of "0" because of n=2r. In consequence, the slot error rate is equal to the bit error rate (*BER*) of on-off keying (OOK) modulation as

$$P_e = Q\left(\sqrt{SNR}\right). \tag{16}$$

From Eqs.(15) and (16), we can get that

$$P_s = 1-[1-Q(\sqrt{SNR})]^n \,. \tag{17}$$

Fig.7 shows the *SER* of (4, 2) MPPM in the Gaussian channel. From Fig.7, we can see that the simulation results are consistent with the theoretical analysis. Furthermore, we can see that in order to maintain the *SER* less than 10^{-3}, the *SNR* should be larger than 10.8 dB. Fig.8 shows the *SER* of (n, r) MPPM, we can see that the *SER* performance will decrease when the number of slot increases. Accordingly, it is necessary to consider the *SER* performance when choosing the proper (n, r) MPPM in different locations.

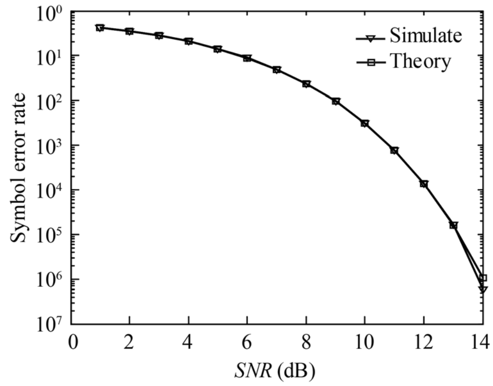

Fig.7 The *SER* of (4, 2) MPPM

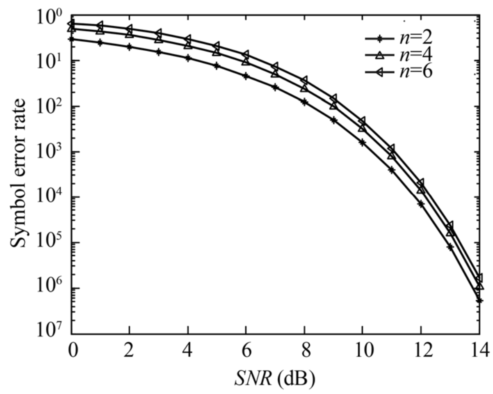

Fig.8 The *SER* of (*n*, *r*) MPPM

We get the best (n, r) MPPM based on the step-by-step method which is shown in detail in the Algorithm 1. The output n represents that the modulation in this position can use (n, n/2) MPPM modulation to get the best data rate. Fig.9 shows the distribution of the proper number of slots n in the case of *SER* less than 10^{-3}. From Fig 9, we can know that n=6 in the position (4.5, 4.5, 0.85), which means that (6, 3) MPPM is the proper modulation for achieving a higher data rate in this position under guarantee of *SER* less than 10^{-3}. For the fixed MPPM, the modulation depends on the minimum *SNR* in order to satisfy the communication quality for every location. In this paper, it can only use (2, 1) MPPM for our environment if we apply the fixed MPPM. It is obvious that the variable MPPM can suit well in the nonuniform indoor channel.

Algorithm 1

Input
Th_{SER}: *SER* threshold
Initialization
i: The number of slots in one MPPM symbol, i = 2
z = 1
While (z)
    $i = i + 2$
    Get the P_s by solve Eq.(15)
    If $P_s > Th_{SER}$
        $i = i - 2$
        $z = 0$
    End
End
$n = i$
Output n

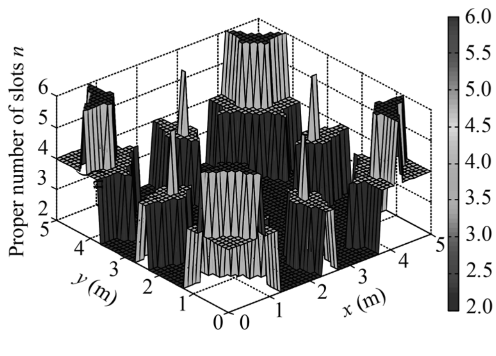

Fig.9 The distribution of the number of *n* with *SER*<10^{-3}

In summary, in this paper, we show that the distribution of *SNR* is nonuniform due to the optical paths from LEDs to the receiver are different. To solve this problem and achieve a high data rate in every location, we propose the location-adaptive transmission scheme based on variable MPPM for the indoor VLC system. To maintain the *SER* less than 10^{-3}, we get the best (n, r) MPPM and achieve the distribution of n by simulation. It is clear that the variable MPPM can achieve higher data rate than the fixed MPPM. Therefore, the location-adaptive transmission scheme based on variable MPPM is an efficient transmission way which can suit well in the nonuniform indoor channel.

References

[1] Yu Hai-feng, Chi Xue-fen and Liu Jian, Optoelectronics Letters **10**, 365 (2014).

[2] Deng Rui, Fan Qi-rui, Dong Huan, He Jing and Chen Lin, Journal of Optoelectronics·Laser **26**, 877 (2015). (in Chinese)

[3] T. Komine and M. Nakagawa, IEEE Transactions on Consumer Electronics **50**, 100 (2004).

[4] Ding J., Huang Z. and Ji Y., Journal of the Optical Society of America A **29**, 971 (2012).

[5] Jupeng Ding, Zhitong Huang and Yuefeng Ji, IEEE Communications Letters **16**, 439 (2012).

[6] A. Burton, H. Le Minh, Z. Ghasemlooy and S. Rajbhandari, A Study of LED Lumination Uniformity with Mobility for Visible Light Communications, International Workshop on Optical Wireless Communications, 1 (2012).

[7] Chow C. W., Yeh C. H., Liu Y. F., Huang P. Y. and Liu Y., Optics Communications **292**, 49 (2013).

[8] Lang Lei and Jia Qian, Journal of Optoelectronics·Laser **26**, 81 (2015). (in Chinese)

[9] Rajbhandari S., Chun H., Faulkner G., Cameron K., Jalajakumari A. V. N., Henderson R., Tsonev D., Ijaz M., Zhe Chen, Haas H., Enyuan Xie, McKendry J. J. D., Herrnsdorf J., Gu E., Dawson M. D. and O'Brien D., IEEE Journal on Selected Areas in Communications **33**, 1750 (2015).

[10] M. Biagi, T. Borogovac and T. D. C. Little, Journal of Lightwave Technology **31**, 3676 (2013).

[11] J. M. Garrido-Balsells and A. Puertanotario, IET Electronics Letters **42**, 43 (2006).

[12] LIU Yang and ZHANG Guo-an, Optoelectronics Letters **10**, 273 (2014).

[13] Ozaki T., Kozawa Y. and Umeda Y., Improved Error Performance of Variable PPM for Visible Light Communication, International Symposium on Wireless Personal Multimedia Communications (WPMC), 259 (2014).

[14] Petr Chvojka, Stanislav Zvanovec, Paul Anthony Haigh and Zabih Ghassemlooy, Journal of Lightwave Technology **33**, 1719 (2015).

[15] Nakagawa M., Tanaka Y., Komine T. and Haruyama S., IEICE Transactions on Communications **86**, 2440 (2003).

[16] G. Ntogari, T. Kamalakis, J. Walewski and T. Sphicopoulos, Journal of Optical Communications and Networking **3**, 56 (2011).